# Dimerization of the Extracellular Domain of the Erythropoietin (EPO) Receptor by EPO: One High-Affinity and One Low-Affinity Interaction

**ARTICLE** *in* BIOCHEMISTRY · MARCH 1996

Impact Factor: 3.02 · DOI: 10.1021/bi9524272 · Source: PubMed



**5 AUTHORS**, INCLUDING:

John S Philo
Alliance Protein Laboratories
**102** PUBLICATIONS **3,666** CITATIONS
SEE PROFILE

Tsutomu Arakawa
**384** PUBLICATIONS **15,984** CITATIONS
SEE PROFILE

# Dimerization of the Extracellular Domain of the Erythropoietin (EPO) Receptor by EPO: One High-Affinity and One Low-Affinity Interaction

John S. Philo,* Kenneth H. Aoki, Tsutomu Arakawa, Linda Owers Narhi, and Jie Wen

*Protein Chemistry Department, Amgen, Inc., Amgen Center, Thousand Oaks, California 91320*

*Received October 10, 1995; Revised Manuscript Received December 6, 1995*[⊗]

ABSTRACT: Although there is considerable evidence that signaling by the erythropoietin (EPO) receptor is initiated when it is dimerized by binding EPO, it has been previously reported that the soluble extracellular domains of the EPO receptor (sEPOR) are not dimerized in the presence of EPO and are able to form only 1:1 complexes with EPO. We have now shown unambiguously by light scattering, sedimentation equilibrium, and titration calorimetry that two molecules of sEPOR can bind to a single EPO monomer but that the binding of the second sEPOR is ~1000-fold weaker than that of the first. Because this second binding interaction is quite weak ($K_d$ of ~1 $\mu$M), the 2:1 sEPOR·EPO complexes are easily dissociated during chromatography (forming the 1:1 complexes reported previously) and cannot be isolated in pure form. Global analysis of the sedimentation equilibrium data has enabled us to determine the binding constants and is consistent with a model in which EPO has two independent binding sites for sEPOR but cannot exclude anticooperative or sequential binding models. The influence of glycosylation of EPO and/or sEPOR on the binding affinities has also been investigated. Titration calorimetry is consistent with the sedimentation data and shows that the weaker binding site has a more negative $\Delta H$. The relation of these results to the binding of EPO to membrane-bound receptors and to the phenomenon of apparent high-affinity and low-affinity classes of receptors is discussed.

Significant progress has recently been made in understanding the signaling pathways in erythroid cells which occur subsequent to the binding of erythropoietin (EPO),[1] the primary regulator of erythropoiesis. The erythropoietin receptor (EPOR), like other cytokine receptors, lacks a tyrosine kinase in its cytoplasmic domain. Nonetheless, binding of EPO to the cell surface does induce phosphorylation of EPOR itself, and of the tyrosine kinase JAK2, which physically associates with a membrane-proximal region of the EPOR cytoplasmic domain (Witthuhn, 1993; Ihle *et al.*, 1994; Sawyer, 1994a; Miura *et al.*, 1994; Yi *et al.*, 1995). Other proteins involved in EPO signal transduction are Ras, Raf1, ERK1, and ERK2 (Todokoro *et al.*, 1994) as well as the phosphatases PTP1C (SH-PTP1) and Syp (SH-PTP2) (Tauchi *et al.*, 1990; Yi *et al.*, 1995; Klingmüller *et al.*, 1995).

Despite these recent gains in understanding intracellular signaling pathways, the mechanism by which the binding of EPO to the extracellular domain of its receptor triggers this signal transduction cascade remains unclear. Ligand-induced receptor oligomerization is widely believed to be the mechanism which initiates signal transduction for all the cytokine receptors. Some members of this receptor family, such as the growth hormone receptor, are known to form homodimers upon ligand stimulation (Cunningham *et al.*, 1991), while others such as the receptors for interleukin-3 and granulocyte-macrophage colony-stimulating factor form heterodimers (Miyajima *et al.*, 1993). The growth hormone receptor has been particularly well-characterized (de Vos *et al.*, 1992; Fuh *et al.*, 1992; Clackson & Wells, 1995), and the same homodimerization mechanism is often assumed to occur for other cytokine receptors, including EPOR (Ihle *et al.*, 1994; Heldin, 1995).

In fact, for EPO and EPOR, there is evidence both for and against a receptor homodimerization mechanism. The observation that a mutant EPOR which is covalently dimerized by interchain disulfide bonds is constitutively active and renders cells factor-independent provides strong evidence that EPOR homodimerization is sufficient to initiate signal transduction (Watowich *et al.*, 1992). Further support for the homodimerization model comes from the dominant inhibitory effect observed when signaling-incompetent EPOR mutants truncated in the cytoplasmic domain are coexpressed with wild-type EPOR (Watowich *et al.*, 1994), although the opposite result has also been reported (Miura & Ihle, 1993a).

On the other hand, two other groups have reported that soluble extracellular domains of EPOR (sEPOR) are not dimerized by EPO, but instead form only 1:1 complexes with EPO, on the basis of SEC and cross-linking studies, and that the binding affinity of sEPOR appears to be too low to account for the high-affinity binding sites typically found on EPO-responsive cells (Nagao *et al.*, 1992; Yet & Jones, 1993). Further, Miura and Ihle (1993b) found that a substantial fraction of EPOR exists as dimers or oligomers even in the absence of EPO, due at least in part to intermolecular disulfide bonds. Additional evidence against a homodimerization mechanism is that a number of groups have reported that high-affinity binding of EPO requires the presence of another cellular component in addition to EPOR (Dong & Goldwasser, 1993; Masuda *et al.*, 1993; Nagao *et al.*, 1993). Taken together, these latter results seem consistent with a view that the true high-affinity EPO receptor may

* To whom correspondence should be addressed.

[⊗] Abstract published in *Advance ACS Abstracts,* January 15, 1996.

[1] Abbreviations: EPO, human erythropoietin; CHO EPO, glycosylated erythropoietin produced by expression in Chinese hamster ovary cells; *E. coli* EPO, unglycosylated erythropoietin produced by expression in *Escherichia coli*; sEPOR, the soluble extracellular domain of the erythropoietin receptor; PBS, Dulbecco's phosphate-buffered saline (pH 7.0); SEC, size exclusion chromatography.

0006-2960/96/0435-1681$12.00/0 

be a heterodimer (or higher oligomer) containing EPOR and a second (unknown) protein.

In summary, at present there is conflicting evidence regarding a homo- or heterodimerization mechanism for EPOR. We have therefore carried out new studies to characterize the binding of EPO to the soluble extracellular domain of EPOR using three biophysical techniques not previously employed on this system: sedimentation equilibrium, titration calorimetry, and size exclusion chromatography with on-line light-scattering detection. All three techniques clearly show that EPO is capable of dimerizing sEPOR in solution. Further, we have shown that the second sEPOR binds to EPO with about a 1000-fold lower affinity than does the first sEPOR and have investigated how glycosylation of ligand and/or receptor alters these binding interactions. Lastly, we discuss the issue of whether the binding behavior of the extracellular domain is sufficient to account for the binding affinity and EPO activation of the holoreceptor in a cell membrane.

## MATERIALS AND METHODS

*Materials.* Recombinant CHO cell-derived EPO was purified from the CHO-conditioned media using anion exchange, reversed phase, and size exclusion chromatography, using a procedure described previously (Takeuchi *et al.*, 1989). Recombinant *Escherichia coli*-derived EPO was purified as described previously (Narhi *et al.*, 1991). Recombinant sEPOR was purified from CHO cell-conditioned media by anion exchange and hydrophobic interaction chromatography and ammonium sulfate precipitation. Deglycosylated sEPOR was obtained by treating the glycosylated sEPOR with *N*-glycanase (Genzyme) for 16 h at 37 °C. A molar extinction coefficient of $2.26 \times 10^4$ $M^{-1}$ $cm^{-1}$, based on dry-weight measurements of CHO EPO (Davis *et al.*, 1987), was used for all forms of EPO; for EPOR, a value of $4.1 \times 10^4$ $M^{-1}$ $cm^{-1}$ was calculated from the amino acid composition (Gill & von Hippel, 1989).

*Light-Scattering/Size Exclusion Chromatography.* The on-line light-scattering/chromatography system uses three detectors in series: an absorbance monitor at 280 nm (Knauer A293), a laser light-scattering detector (Wyatt Mini-Dawn), and a refractive index detector (Polymer Laboratories PL-RI). For these experiments, a Superdex 200 (Pharmacia) column was used with PBS as the elution buffer at a flow rate of 0.5 mL/min. Procedures, calibration, and methods of data analysis for receptor·ligand complexes followed those described previously (Philo *et al.*, 1994). The molecular weights of the polypeptide component of glycoproteins or complexes were calculated from the relation

$$M = K(\mathrm{LS})(\mathrm{UV})/[\epsilon(\mathrm{RI})^2]$$

where (LS), (UV), and (RI) are the signals from the 90° light-scattering, absorbance, and refractive index detectors, respectively, $\epsilon$ is the absorbance of a solution containing 1 mg of polypeptide per milliliter with a path length of 1 cm, and $K$ is a calibration constant.

*Titration Calorimetry.* Data were collected at 25 °C using either Microcal Omega (Northhampton, MA) or Calorimetry Sciences (Provo, UT) calorimeters. Protein solutions for calorimeter cells and injection syringes were dialyzed into the same buffer to minimize heats due to solvent mismatch. PBS was used for experiments with CHO EPO, while PBS + 1% polyethylene glycol 1000 (Baker) was used with *E. coli* EPO to enhance its solubility. Data were analyzed using either the Microcal Origin program (version 2.8) or the program TITRATE written in-house, which uses identical fitting functions but gives more rigorous estimates of the confidence intervals for the parameters. Since control injections of EPO into buffer showed no significant heat of dilution, and all experiments gave non-zero heats for injections after the binding phase is complete, the analysis included a fitting term adding a constant heat per injection due to a slight mismatch in buffer composition or temperature between the cell and the solutions in the syringe.

*Sedimentation Equilibrium.* Sedimentation equilibrium experiments were carried out at 25 °C using six-channel charcoal-Epon cells in a Beckman XL-A analytical ultracentrifuge. Concentration distributions were measured at 280 or 230 nm. Samples were equilibrated at each speed for at least 24 h, and attainment of equilibrium was verified by the constancy of scans taken 4 h apart. At the conclusion of a run, the rotor was taken to 48 000 rpm for >18 h to force all the protein to the bottom of the cell. Scans of the upper portions of each channel at this high speed were used to establish a base line absorbance level for each sample, and this base line offset was subtracted from the data before further processing. In cases where the high-speed data showed significant base line deviations due to dirt or scratches on the windows, these data were used to create a base line file, which was then shifted radially to correct for differences in the radial expansion of the rotor and subtracted from the experimental data at lower speeds.

The sedimentation data on the mixtures were fitted to heterogeneous association models of the forms $A + B \leftrightarrow AB$ or $A + 2B \leftrightarrow AB + B \leftrightarrow AB_2$, where A is EPO, and B is sEPOR, accounting for the different molar extinction coefficients of each species at the measurement wavelength, using techniques described previously (Philo *et al.*, 1994). During fitting, the buoyant molecular weight of each monomeric species was held fixed at the value determined when it was run alone (for glycosylated proteins) or at the value calculated from the sequence $M_r$ (for nonglycosylated proteins). The data for up to 18 samples were globally fitted to determine the association constants. During fitting, the fitted parameters were constrained to values which account for the total concentration of each protein in the cell ±10%.

A density of 1.003 99 g/mL for PBS was measured with a Mettler-Paar DMA-02 density meter. Polypeptide partial specific volumes of 0.7418 and 0.7353 mL/g for *E. coli* EPO and EPOR, respectively, were calculated from their amino acid composition (Laue *et al.*, 1992).

## RESULTS

### *SEC with Light-Scattering Detection*

In earlier studies of the stoichiometry of sEPOR binding to EPO, SEC was used to estimate the molecular weight of sEPOR·EPO complexes on the basis of their elution positions (Nagao *et al.*, 1992; Yet & Jones, 1993). However, in addition to molecular weight, SEC elution positions are affected by molecular shape (which may alter upon formation of complexes) and nonspecific interactions with the column, and an accurate molecular weight calibration for glycoproteins is exceedingly difficult. Our approach is instead to use SEC with on-line light-scattering, refractive index, and absorbance detectors, which enables us to determine the

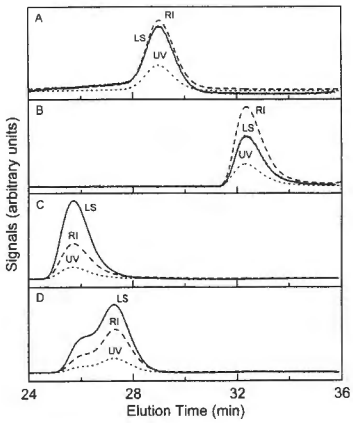


FIGURE 1: SEC chromatograms for EPO, sEPOR, and mixtures. Signals are shown for the light-scattering (LS, solid line), refractive index (RI, dashed line), and absorbance (UV, dotted line) detectors: (A) glycosylated sEPOR, (B) *E. coli* EPO, (C) a mixture of sEPOR and EPO at a 2:1 molar ratio (8.64 mg/mL sEPOR + 3.18 mg/mL EPO), and (D) a mixture of sEPOR and EPO at a 1:1 molar ratio (4.32 mg/mL sEPOR + 3.18 mg/mL EPO).

polypeptide molecular weights of glycoproteins and complexes independently of their elution position (Takagi, 1990; Arakawa *et al.*, 1994; Philo *et al.*, 1994).

The results from these experiments are summarized in Figure 1 and Table 1. We first injected glycosylated sEPOR and *E. coli* EPO separately (Figure 1A,B), which gave light-scattering molecular weights of 24 000 ± 1000 and 19 000 ± 1000, respectively, for their polypeptide components, consistent with their sequence molecular weights. We next injected mixtures of sEPOR and EPO made at high protein concentrations (8−12 mg/mL) and at approximately 2:1 or 1:1 sEPOR:EPO stoichiometry (Figure 1C,D, respectively). In both cases, essentially all the proteins are eluted as protein complexes. For the 2:1 sample, the complexes elute as a single peak. Only a trace amount of free receptor is present in this 2:1 sample, which strongly suggests that 1 mol of EPO is capable of binding 2 mols of receptor and also that essentially all the sEPOR is competent for EPO binding. The 1:1 sample shows two poorly resolved peaks of protein complexes: a minor one at the same elution position as that of the 2:1 sample and a second major peak at a position intermediate between the first peak and that for the free receptor. A small amount of free EPO is also present in the 1:1 sample.

One complication in the determination of the molecular weight of these complexes is the fact that our three-detector calculation method requires the extinction coefficient, $\epsilon$, of the complex (see Materials and Methods). Since the $\epsilon$ values for sEPOR and EPO are different, the correct $\epsilon$ value for a sEPOR·EPO complex depends on its stoichiometry (which is what we are trying to determine). This apparent dilemma is solved by an iterative method. First, the correct extinction coefficient and theoretical molecular weight for various plausible stoichiometries are calculated, and then each of these values are used to calculate an apparent molecular weight from light scattering. Each possible stoichiometry is then tested for self-consistency between the theoretical and experimental molecular weight, and that stoichiometry which gives the best self-consistency is accepted as the correct one. The results of such self-consistency tests for the sEPOR + EPO mixtures are summarized in Table 1. The data for the 2:1 mixture are most consistent with a two sEPOR per EPO stoichiometry, as are those for the earlier eluting peak in the 1:1 mixture. The second peak in the 1:1 mixture, on the other hand, is in excellent agreement with a 1:1 stoichiometry.

The light-scattering molecular weights for the 2:1 complexes are, however, somewhat lower than the expected theoretical value. In the case of the small 2:1 component in the 1:1 mixture, this is likely a result of the poor chromatographic separation between 2:1 and 1:1 complexes. For the 2:1 mixture, however, the molecular weight is probably slightly lower than expected for 2:1 complexes because the binding affinity is low enough that there is some dissociation into 1:1 complexes. That is, this chromatographic peak probably represents a dynamic equilibrium sEPOR·EPO·sEPOR ↔ sEPOR·EPO + sEPOR in which the kinetics are rapid enough that all three different species are present but not chromatographically separated, thus producing an average molecular weight lower than that of a pure 2:1 complex. In fact, when the protein concentration is lowered, the results are quite different. Figure 2 shows the absorbance chromatograms when the same 2:1 and 1:1 mixtures are diluted 10- or 50-fold prior to injection, as compared to the data at high concentrations. For the 2:1 mixture, upon dilution, the elution position continues to shift toward that of the 1:1 complex, but no resolution into two peaks is seen, consistent with a dynamic equilibrium. The relative amount of the free receptor peak also increases significantly as the concentration is lowered. For the 1:1 mixture, the minor 2:1 complex peak is nearly gone at 10-fold dilution, but the peak from 1:1 complexes remains at the same position. Together, these observations suggest that the 2:1 complex is much more easily dissociated than the 1:1 complex; *i.e.* the binding of a second receptor to the same EPO molecule may be much weaker than the binding of the first.

### *Sedimentation Equilibrium*

*Deglycosylated sEPOR + E. coli EPO.* While the light-scattering data are consistent with dimerization of sEPOR by EPO at high protein concentrations, sedimentation equilibrium is a more powerful method for exploring the details of these interactions. Our initial sedimentation equilibrium studies employed *E. coli* EPO and deglycosylated sEPOR in order to avoid the inherent heterogeneity of glycosylation. First, it is essential to know whether sEPOR shows any tendency to dimerize in the absence of EPO. Control studies gave excellent fits with sEPOR as a single, ideal species. The quantity directly measured in sedimentation equilibrium is the buoyant molecular weight, $M_r(1 - \bar{\nu}\rho)$, where $\bar{\nu}$ is the protein's partial specific volume and $\rho$ is the solvent density. From the fitted buoyant molecular weight of 6543 (95% confidence interval 6485 to 6608), the calculated $\bar{\nu}$, and the measured $\rho$, this data give a protein $M_r$ = 24 949 [24727−25195].[2] Since this confidence interval includes the sequence molecular weight of 24 750, the data are fully consistent with no self-association to dimers or higher oligomers. Thus, both our sedimentation equilibrium and SEC data fail to show that small amounts of sEPOR dimers exist in the absence of EPO as was reported by Yet and Jones (1993). Control studies of *E. coli* EPO were also consistent with a single species at its sequence $M_r$ of 18 392.

We have studied mixtures of sEPOR with *E. coli* EPO made at stoichiometries from 4:1 to 1:1 sEPOR:EPO, with

[2] Hereafter, 95% confidence intervals for fitted values will be shown within square brackets.

Table 1: Summary of Light-Scattering Results

| proteins or complexes | assumed, stoichiometry | $\epsilon^a$ (mL mg$^{-1}$ cm$^{-1}$) | molecular weight from light scattering$^b$ ± 5% | theoretical molecular weight$^c$ | correct assumption? |
|---|---|---|---|---|---|
| *E. coli* EPO | – | 1.24 | 19 000 | 18 400 | – |
| glycosylated sEPOR | – | 1.66 | 24 000 | 24 750 | – |
| mixture 1 (two sEPOR per EPO) | | | | | |
| peak at $t = 25.5$ min | 1 sEPOR: 1 EPO | 1.48 | 64 000 | 43 150 | no |
| | 2 sEPOR: 1 EPO | 1.55 | 61 000 | 67 900 | yes |
| mixture 2 (one sEPOR per EPO) | | | | | |
| peak 1 ($t = 25.8$ min) | 1 sEPOR: 1 EPO | 1.48 | 63 000 | 43 150 | no |
| | 2 sEPOR: 1 EPO | 1.55 | 60 000 | 67 900 | yes |
| peak 2 ($t = 27.2$ min) | 1 sEPOR: 1 EPO | 1.48 | 44 000 | 43 150 | yes |
| | 2 sEPOR: 1 EPO | 1.55 | 42 000 | 67 900 | no |

[a] Excluding carbohydrate. [b] Excluding carbohydrate. [c] Calculated from sequence molecular weights.

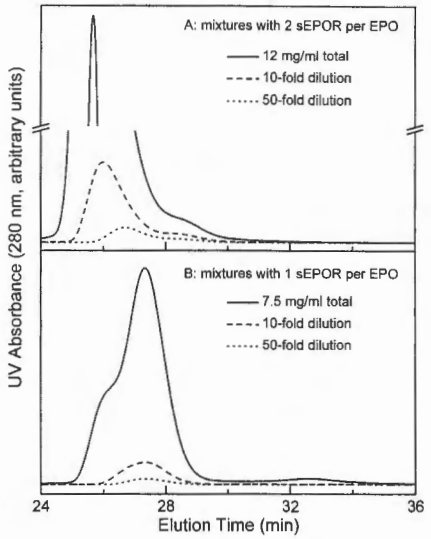


FIGURE 2: Concentration dependence of SEC chromatograms. Only the absorbance signal is shown: (A) (1) mixture 1 from Figure 1C, glycosylated sEPOR + *E. coli* EPO at a 2:1 molar ratio, 11.8 mg/mL total protein (solid line); (2) 10-fold dilution of mixture 1 (dashed line); and (3) 50-fold dilution of mixture 1 (dotted line); (B) (1) mixture 2 from Figure 1D, sEPOR + EPO at a 1:1 molar ratio, 7.5 mg/mL total protein (solid line); (2) 10-fold dilution of mixture 2 (dashed line); and (3) 50-fold dilution of mixture 2 (dotted line).

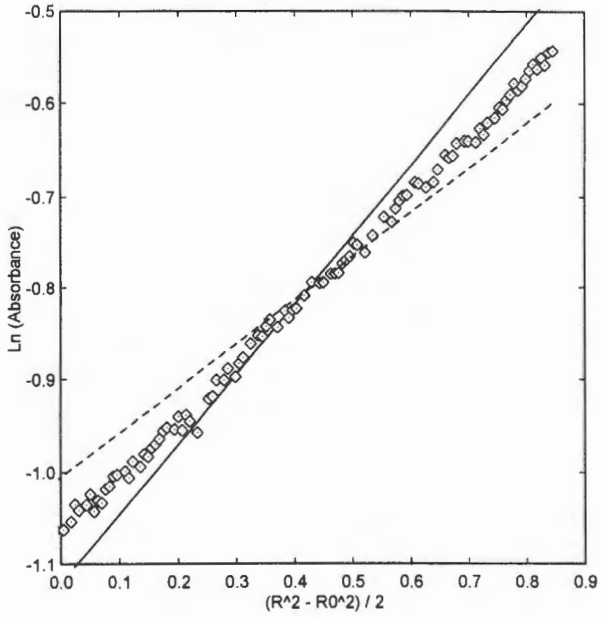


FIGURE 3: Sedimentation equilibrium of 6 $\mu$M deglycosylated sEPOR + 3 $\mu$M *E. coli* EPO at 10 000 rpm. The natural log of the absorbance at 280 nm is plotted *versus* $(r^2 - r_o^2)/2$, where $r$ is the radius and $r_o$ is the radius at the center of the sample. In this type of plot, a single species will give a straight line whose slope is proportional to molecular weight. The solid line illustrates the slope calculated for a complex of two sEPOR per EPO. The dashed line illustrates the slope for a complex of one sEPOR per EPO. Only data for the outer half of the sample (which will contain the highest molecular weight species) are shown.

sEPOR loading concentrations from 1 to 6 $\mu$M, and at several rotor speeds. Some data for a 2:1 mixture are plotted in a simple way in Figure 3. For a single species, such a plot will give a straight line whose slope is directly proportional to molecular weight, while for a mixture of species, the slope near the outside of the rotor will be dominated by the species of highest molecular weight. The solid and dotted lines indicate the predicted slopes for 2:1 and 1:1 sEPOR·EPO complexes, respectively. The fact that the slope is greater than the value for a 1:1 complex clearly indicates that some 2:1 complexes are present, but the fact that the slope is also well below that for 2:1 complexes indicates that formation of this type of complex is incomplete.

For a more detailed, quantitative analysis, multiple sedimentation equilibrium experiments were globally fitted to various binding models. During the fitting, constraints were imposed to make the fitted species distributions match the ratio of sEPOR to EPO placed into the centrifuge cell within ±10%. Consistent with our interpretation of Figure 3, fits of the data to a model in which only one sEPOR can bind per EPO are very poor (not shown). Furthermore, with a 1:1 binding model, the fitting routine tries to make the binding infinitely strong to maximize the molecular weight.

Turning to models where two receptors can simultaneously bind to EPO, there are four possible thermodynamic models to consider: (1) the two binding sites on EPO have equivalent affinities, (2) the two sites have fixed, inequivalent affinities, (3) the two sites are initially equivalent but interact cooperatively, or (4) the two sites are inequivalent and also interact cooperatively (for the cooperative models, it is important to note that it is irrelevant for this analysis whether cooperativity arises through receptor−receptor interactions, conformational changes in EPO, or both). Since EPO has no known internal symmetry, it seems unlikely that the two sites would be energetically equivalent, and indeed, fits to the two-equivalent site model are quite unsatisfactory.

We obtain excellent fits to a model with two independent, nonequivalent binding sites. Figure 4 shows an overlay of the data and fitted curves, and the residuals, for the global analysis of nine samples (three concentrations each at 2:1, 4:3, and 1:1 sEPOR:EPO ratios) at two rotor speeds. Clearly, this model provides a very good fit to all 18 experiments. The best fit dissociation constants from this analysis are 0.36

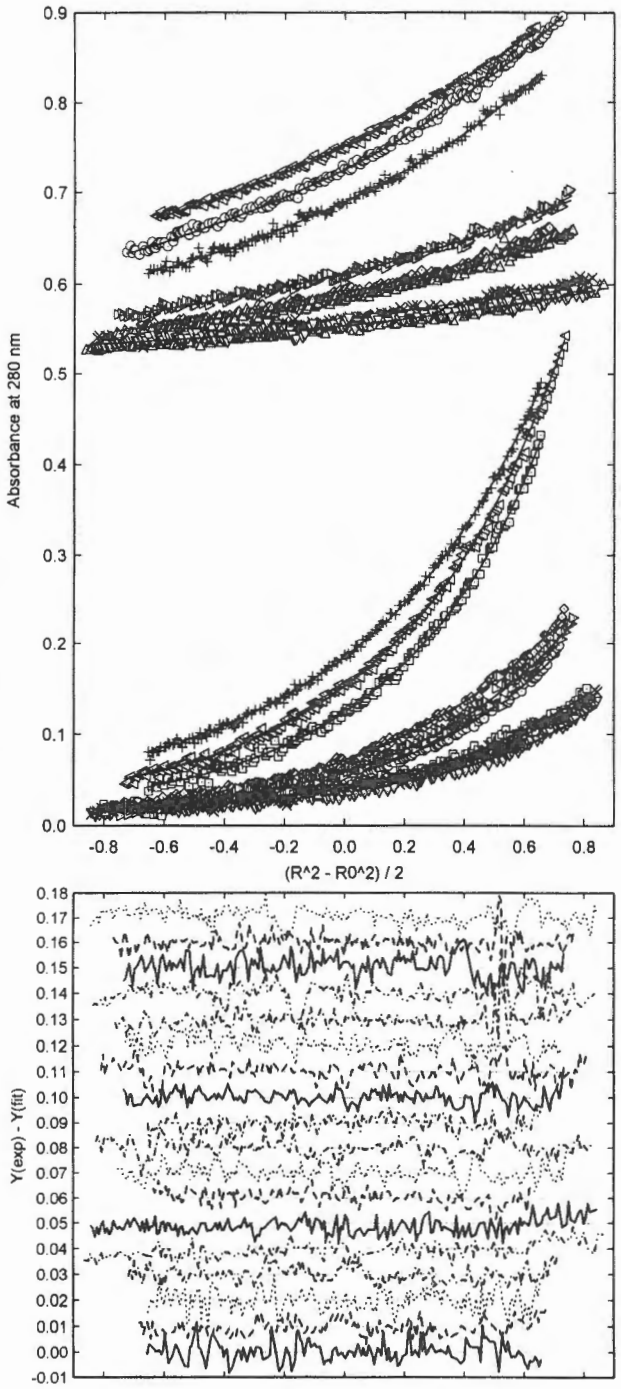


FIGURE 4: Sedimentation equilibrium data, fitted curves, and residuals for deglycosylated sEPOR + *E. coli* EPO mixtures. Data for nine samples were recorded at 10 000 and 18 000 rpm and globally fitted to a binding model where each EPO molecule can bind two sEPOR molecules at two independent sites with different affinities. The upper panel shows the raw data and the fitted curves with dissociation constants of 0.36 nM and 1.09 $\mu$M. The data sets at 10 000 rpm have been shifted upward by 0.5 absorbance unit for the sake of clarity. The lower panel shows the residuals (experimental minus fitted values) for all 18 data sets, with each successive data set shifted vertically by 0.01 absorbance unit to reduce overlap. The overall root mean square deviation for the 2706 data points is 0.0049 absorbance unit.

nM and 1.09 $\mu$M, *i.e.* the two sites are ~3000-fold different in affinity. The $K_d$ of the weaker binding site (which we will hereafter call site 2) is well-determined, with a 95% confidence interval from 0.85 to 1.35 $\mu$M. The affinity of the strong binding site (site 1) is so high compared to that of site 2 that it is not well-determined from these data (which must necessarily be run at relatively high protein concentrations if we want to see both types of interaction), so the 95% confidence interval for the $K_d$ of site 1 ranges from 0 to 3.4 nM. The analysis of a second set of experiments (14 data sets) gave similar and consistent results: a site 2 dissociation constant of 0.92 [0.70−1.17] $\mu$M and again a poorly determined $K_d$ of ~0.5 nM for site 1.

The rather weak binding to site 2 explains the dissociation of the 2:1 complex when the SEC samples were diluted. The large difference in binding affinity between sites 1 and 2 also explains why the 1:1 complex predominates in samples made at 1:1 stoichiometry (Figure 1D), since it will be energetically more favorable for sEPOR molecules to bind to site 1 than to site 2 whenever sufficient numbers of type 1 sites are available. Indeed, it is primarily this competition between binding to site 1 or site 2 that makes the distribution of species in the sedimentation equilibrium samples sensitive to the site 1 affinity even at high protein concentrations.

While the two-nonequivalent independent site model appears sufficient to explain these data in detail, it is not the only two-site model that can do so. For example, the data can be fitted equally well by a model with two equivalent sites with a strong negative cooperativity that reduces the $K_d$ from ~1 nM for binding the first sEPOR to ~1 $\mu$M for binding the second (in which case what we have been calling "site 1" and "site 2" are not physically unique sites on EPO). For the dimerization of soluble human growth hormone receptor (hGHbp) by human growth hormone (hGH), a model has been proposed in which the second binding site does not exist until the first receptor is bound (Fuh *et al.*, 1992). This sequential binding model is also compatible with these sEPOR data. In fact, this sequential model is virtually indistinguishable from the two-nonequivalent independent site model because for EPO the site 2 affinity is so low compared to that of site 1 that it makes almost no difference whether this site 2 affinity is zero or finite when site 1 is unoccupied. The hGHbp/hGH sequential model is actually a special case of a model with two nonequivalent cooperative sites, in which a strong positive cooperativity greatly increases the affinity of site 2 when site 1 is occupied. The sEPOR/EPO data are also consistent with more general nonequivalent cooperative site models over a broad range of cooperativity, as long as (a) the affinity of site 2 is low when site 1 is unoccupied, (b) the intrinsic affinity of site 1 is high, and (c) the cooperativity produces a $K_d$ of ~1 $\mu$M for site 2 when site 1 is occupied.

*Glycosylated sEPOR and E. coli EPO.* Similar sedimentation equilibrium studies were done using the glycosylated form of sEPOR, which has a single N-linked glycosylation site. Control studies of the sEPOR alone again showed no self-association and were consistent with a single species of buoyant molecular weight of 7233 [7153−7313]. From this value, the sequence molecular weight, and estimates of the carbohydrate partial specific volume, a self-consistent calculation gives a total molecular weight of 26 765 [26097−27395] (Philo *et al.*, 1994), which agrees with laser-desorption mass spectroscopy data (V. Katta, private communication).

Samples were made at both 2:1 and 1:1 sEPOR:EPO stoichiometries and sEPOR concentrations from 4 to 1 $\mu$M and run at three rotor speeds, for a total of 16 data sets. The two-nonequivalent independent binding site model again provides an excellent global fit to all these data and returns dissociation constants of 0.70 [0.64−0.77] $\mu$M for site 2 and 2.6 [0.56−3.9] nM for site 1. The high site 1 affinity is

indistinguishable from that for the nonglycosylated receptor, while the site 2 affinity appears to be marginally higher when the receptor is glycosylated.

*Glycosylated sEPOR and CHO EPO.* Since CHO EPO is heavily glycosylated (~40% carbohydrate), it is of interest to know whether this significantly alters the interactions with the soluble receptor. Earlier sedimentation equilibrium studies of EPO showed it to behave essentially as a single species of $M_r = 30\,400 \pm 400$, with a small nonideality observable at higher loading concentrations (~0.6 mg/mL) (Davis *et al.*, 1987). New studies of CHO EPO at 36 $\mu$g/mL were consistent with these earlier studies, giving $M_r = 30\,460$ [30340−30570] using the experimental $\bar{\nu}$ (Davis *et al.*, 1987). If instead we use a calculated polypeptide $\bar{\nu}$, estimated carbohydrate $\bar{\nu}$ and the self-consistent analysis, the results are very similar, giving $M_r = 30\,390$ [29150−31080].

Ten data sets for sEPOR + EPO mixtures were again well fitted by the two-nonequivalent independent binding site model. The data, fitted curves, and residuals from this fit, which returned $K_d$s of 0.2 [0−2.8] nM and 2.1 [1.6−2.6] $\mu$M for sites 1 and 2, respectively, are shown in Figure 5. These values, and those found with one nonglycosylated protein, are summarized in Table 2. A comparison shows glycosylation of the ligand does indeed significantly lower the site 2 affinity (~3-fold), but we are unable to distinguish whether there is a comparable change in the site 1 affinity. Given the inherent heterogeneity of glycosylation, it is therefore likely that glycosylated EPO actually has subpopulations with binding affinities both higher and lower than this value, but the affinities of different glycoforms are similar enough that we can represent the data fairly well by this single affinity. The residuals for this fit do show larger systematic deviations than that for the unglycosylated proteins (Figure 4), but this may be due to the glycosylation-induced spread in the molecular weight of each protein in addition to a possible distribution of affinities.

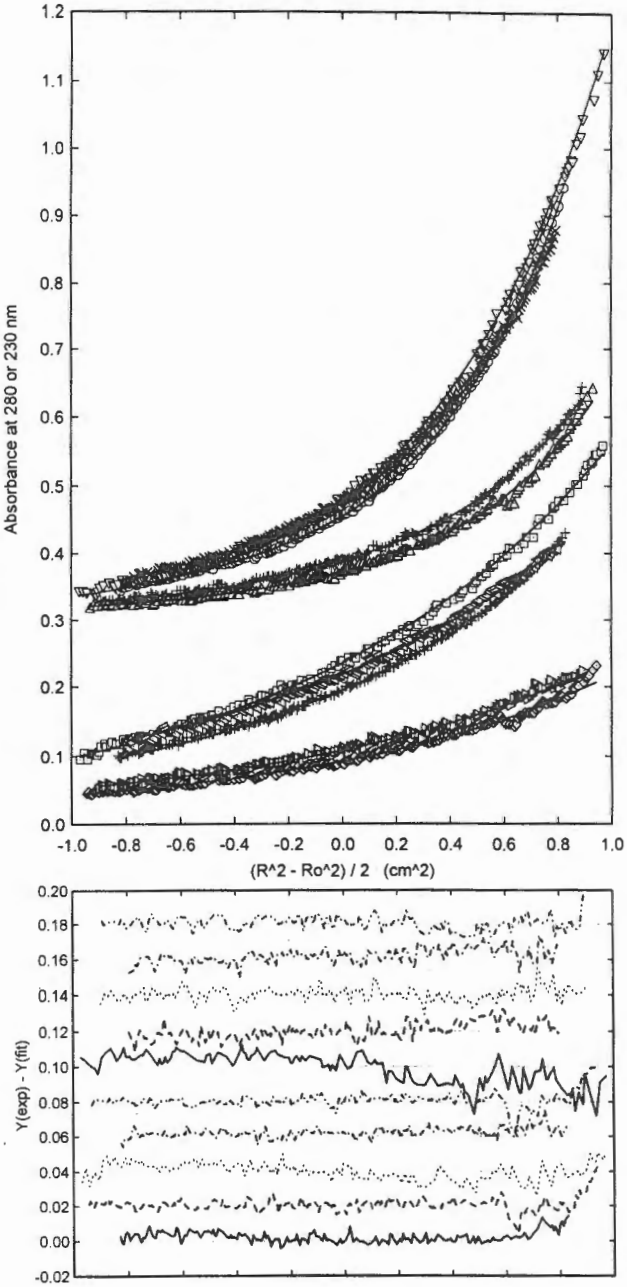


FIGURE 5: Sedimentation equilibrium data, fitted curves, and residuals for glycosylated sEPOR + CHO EPO mixtures. Data for five samples at 11 000 and 15 000 rpm were globally fitted to the two-nonequivalent independent binding site model. The upper panel shows the raw data and the fitted curves with dissociation constants of 0.2 nM and 2.1 $\mu$M for sites 1 and 2. The data sets at 15 000 rpm have been shifted upward by 0.3 absorbance unit for the sake of clarity. Because some samples were scanned at 280 and some at 230 nm, the actual range of protein concentrations is ~5-fold greater than is apparent from the absorbance values. The lower panel shows the residuals for all 10 data sets, with each successive data set shifted vertically by 0.02 absorbance unit to reduce overlap. The overall root mean square deviation for the 1897 data points is 0.0049 absorbance unit.

## *Titration Calorimetry*

Titration calorimetry is an excellent tool for establishing the stoichiometry and binding enthalpies of protein−protein interactions and can also determine binding affinities when they are not too high. Figure 6 shows some data for the titration of glycosylated sEPOR by CHO EPO, plotted such that heat released will produce a positive signal, with the integrated heats from each injection shown in the lower panel. With the protein concentrations and volumes used for this experiment, the overall sEPOR:EPO stoichiometry in the cell will reach 2:1 after approximately 4.5 injections and 1:1 after 9 injections. The striking result of this experiment is that heat is released during the first 5 injections, and absorbed during the next 5, after which a constant small response (similar to that when buffer is mixed with buffer) is seen.

This switch from heat release to absorption during the titration constitutes a diagnostic pattern that can only occur if (a) more than one receptor binds per EPO, (b) the different binding sites on EPO have different affinities, and (c) the binding enthalpy, $\Delta H$, of the weaker site(s) is more negative than that of the stronger. The fact that the switch in sign occurs just beyond the point where a 2:1 stoichiometry is reached is further diagnostic that a maximum of two sEPOR molecules are bound per EPO. This same pattern of heat absorption and release has been found for all combinations of glycosylated and unglycosylated proteins, and using two different types of calorimeter.

These data raise two important questions. First, if the fundamental interaction stoichiometry is 2:1, then after the fourth injection in Figure 6 there is sufficient EPO present to provide binding sites for all the sEPOR. Therefore, during the rest of the titration, all the sEPOR is already bound to EPO, so why is any signal produced thereafter, let alone a negative one? Second, does the heat absorption phase imply

Table 2: Dissociation Constants Determined by Sedimentation Equilibrium (25 °C, PBS)

| proteins | $K_d$ (site 1) (nM) | $K_d$ (site 2) ($\mu$M) |
|---|---|---|
| deglycosylated sEPOR + *E. coli* EPO | 0.36 [0−3.4] | 1.09 [0.85−1.35] |
| glycosylated sEPOR + *E. coli* EPO | 2.6 [0.56−3.9] | 0.70 [0.64−0.77] |
| glycosylated sEPOR + CHO EPO | 0.2 [0−2.8] | 2.1 [1.6−2.6] |

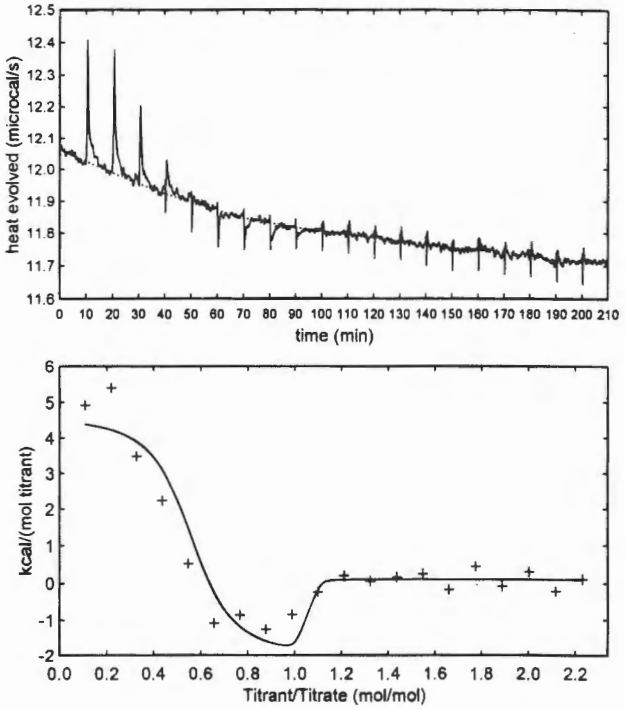


FIGURE 6: Titration calorimetry data for the binding of glycosylated sEPOR to CHO EPO. A 1.36 mL solution of 31.9 mM sEPOR was titrated with 4 $\mu$L injections of 1.18 mM EPO every 10 min in a Microcal Omega calorimeter. The upper panel shows the raw calorimeter data (solid line) and the base line (dotted line). The data are plotted as heat evolved, so an exothermic reaction will produce a positive signal. The lower panel shows the integrated heat from each injection per mole of EPO added and a fitted titration curve for the two independent binding sites model. For the fitted curve, the dissociation constants were held at the values determined by sedimentation equilibrium (Table 2), and the fit returned binding enthalpies of −1.2 kcal/mol for site 1 and −3.3 kcal/mol for site 2. A term adding a constant heat per injection was included in the fitting to allow for the non-zero instrument response after binding is complete, due to a small mismatch in titrant temperature or buffer composition.

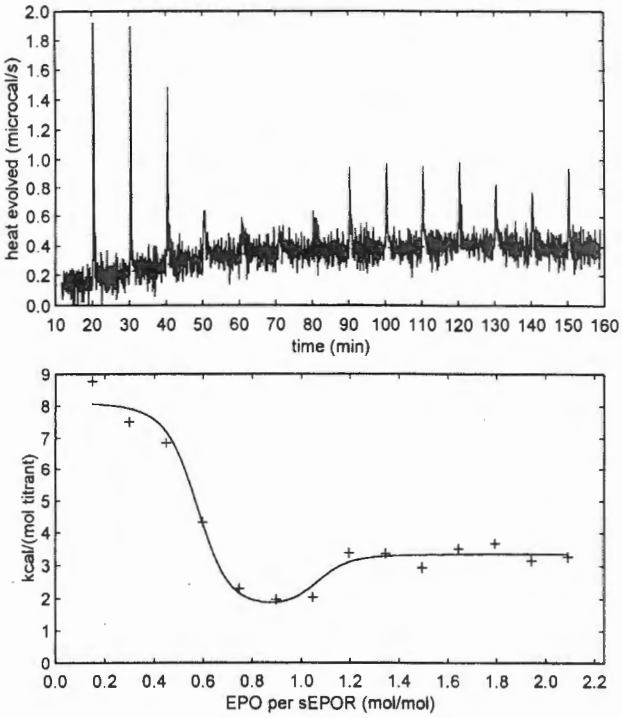


FIGURE 7: Titration calorimetry data for the binding of glycosylated sEPOR to *E. coli* EPO. A 1.0 mL solution of 27.3 mM sEPOR was titrated with 8 $\mu$L injections of 510 $\mu$M EPO every 10 min in a Calorimetry Sciences calorimeter. The upper panel shows the raw calorimeter data (solid line) and the base line (dotted line). These data show a significant constant heat release at each injection which is not due to binding (*i.e.* similar heats are seen for buffer/buffer titrations), and this offset overwhelms the endothermic binding response on injections 5−7. The lower panel shows the integrated heat from each injection per mole of EPO added and a fitted titration curve for the two independent binding sites model. For the fitted curve, the dissociation constants were held at the values determined by sedimentation equilibrium (Table 2), and the fit returned binding enthalpies of −1.5 kcal/mol for site 1 and −3.4 kcal/mol for site 2.

that receptor binding to one of the sites on EPO is actually an endothermic reaction?

The key to understanding both of these questions is the nonequivalence of the two binding sites on EPO. Early in the titration, sEPOR is greatly in excess over the number of EPO binding sites, so most EPO molecules will have two receptors bound. As the ratio of EPO to sEPOR exceeds 0.5, however, the additional EPO added makes new high-affinity sites available. Therefore, it is thermodynamically highly favorable for sEPOR molecules to leave the weak second binding site on EPO in order to occupy the higher affinity site on the newly added EPO molecules. Thus, the net effect is to break a weaker bond to make a stronger one, and the net reaction is sEPOR●EPO·sEPOR + EPO → sEPOR●EPO + sEPOR●EPO, where the symbol ● indicates the stronger (site 1) bond and the symbol · the weaker (site 2) bond. Although the total number of receptor bonds remains constant in this exchange reaction, if the binding enthalpies for the two sites are different, there will be a net gain or loss of heat, and consequently, this process (which is the dominant reaction as the EPO:sEPOR ratio is increased from ~0.5 to ~1.0) will be detectable in the calorimeter. If $\Delta H_1$ is the binding enthalpy for the stronger binding interaction and $\Delta H_2$ is that for the weaker one, then the net enthalpy for the exchange reaction is $\Delta H_1 - \Delta H_2$, which will be positive (endothermic), as seen in Figure 5, whenever $\Delta H_2$ is more exothermic than $\Delta H_1$.

Another feature of these data is that the overall heat released is remarkably small. Since nearly all the EPO added in the first injections will form 2:1 complexes, the integrated heats imply that $\Delta H_1 + \Delta H_2$ is only approximately −5 kcal/mol, which is far less, for example, than the −27 kcal/mol reported for dimerization of hGHbp by hGH (Cunningham *et al.*, 1991). The kinetics of heat production and release are also surprisingly slow, such that the calorimeter does not return to base line readings until ~8 min after the injection for the first few injections. In contrast, the kinetics are much more rapid when *E. coli* EPO is used instead, as shown in Figure 7, but the data are otherwise very similar (in this experiment each injection is producing a constant heat release which largely obscures the endothermic phase). Glycosylation of the receptor, however, has little effect on the data (not shown).

Table 3: Summary of Thermodynamic Parameters for sEPOR Binding to EPO

| | glycosylated sEPOR + *E. coli* EPO | | glycosylated sEPOR + CHO EPO | |
|---|---|---|---|---|
| binding parameter | site 1 | site 2 | site 1 | site 2 |
| $\Delta G°$ (kcal/mol)[a] | −11.7 [−11.5 to −12.6] | −8.40 [−8.34 to −8.45] | −13.2 [−11.7 to −∞] | −7.75 [−7.62 to −7.91] |
| $\Delta H$ (kcal/mol)[b] | −1.5 [−0.8 to −2.1] | −3.4 [−2.8 to −3.9] | −1.2 [−0.5 to 1.9] | −3.3 [−2.5 to −4.1] |
| $T\delta S$ (kcal/mol)[c] | 10.2 [9.4 to 11.8] | 5.0 [4.5 to 5.6] | 11.0 [9.8 to ∞] | 4.5 [3.5 to 5.4] |

[a] From sedimentation equilibrium, $\Delta G° = RT \ln K_d$. [b] From titration calorimetry. [c] From $\Delta G° = \Delta H - T\delta S$.

For a more quantitative analysis, the integrated heats per injection have been fitted to two-site binding models. The curves in the bottom panels of Figures 6 and 7 are fits to the two-independent binding site model, with exactly one of each type of site per EPO, and with the binding constants for each site held fixed at the values found by sedimentation equilibrium (Table 1). The fit for *E. coli* EPO (Figure 7) is fairly good and returns $\Delta H_1 = -1.5$ [−0.8 to −2.1] and $\Delta H_2 = -3.4$ [−2.8 to −3.9] kcal/mol. The fit for the data with CHO EPO (Figure 6) is not as good but gives values which are not significantly different from those for *E. coli* EPO, $\Delta H_1 = -1.2$ [−0.5 to −1.9] and $\Delta H_2 = -3.3$ [−2.5 to −4.1] kcal/mol. The less satisfactory fit for the CHO EPO data may reflect some heterogeneity in binding affinities and/or binding enthalpies for EPO molecules with differing glycosylation. If the binding constants are allowed to vary during the fitting, it is possible to obtain somewhat better fits, but the correlation between parameters is so high that it is not possible to obtain unique affinities from the calorimetry data alone.

Using the binding affinities from sedimentation equilibrium together with the calorimetric enthalpies, we can also estimate the binding entropies, as summarized in Table 3. Binding to both sites 1 and 2 is primarily entropically driven, but the entropy term is much larger and more dominant for site 1 than site 2. Overall, the calorimetry data show unequivocally that two sEPOR molecules can bind to one EPO and that the binding thermodynamics of the two sites are quite different. These data are also quite consistent with the sedimentation equilibrium analysis.

## DISCUSSION

*Comparison to Other Binding Studies with sEPOR.* We have detected 2:1 complexes between sEPOR and EPO by three different physical techniques. These data also show that the affinity of the second binding site is low, and therefore, the 2:1 complex is only formed in significant amounts at relatively high protein concentrations. This latter fact provides a probable explanation of why two other groups have reported that sEPOR can form only 1:1 complexes with EPO on the basis of SEC and cross-linking studies (Nagao *et al.*, 1992; Yet & Jones, 1993). During the binding studies of Yet and Jones (1993), the maximum receptor concentration used was apparently ~42 nM, well below the dissociation constant of site 2. During the cross-linking studies of Nagao *et al.* (1992), the receptor concentration of 3.6 $\mu$M was high enough that 2:1 complex should have been present, but perhaps the 2:1 complex is difficult to cross-link for structural reasons or due to rapid kinetics of association and dissociation. Furthermore, our demonstration that 2:1 complexes are easily dissociated during chromatography explains why both these groups saw only 1:1 complexes by SEC.

The site 1 dissociation constants from sedimentation equilibrium (Table 1) are consistent with the values of 1.1 nM reported for the 1:1 complex by Yet and Jones (1993) and that of 1.5 nM for a fusion of sEPOR to glutathione *S*-transferase (Harris *et al.*, 1992). A much lower affinity ($K_d$ = 17 nM) was reported for human EPO binding to a murine sEPOR (Nagao *et al.*, 1992).

*Comparison with Human Growth Hormone Binding to Its Receptor.* The extensive studies of the interactions of hGH and hGHbp by X-ray crystallography (de Vos *et al.*, 1992), physical techniques (Cunningham *et al.*, 1991), and site-directed mutagenesis (Fuh *et al.*, 1992; Clackson & Wells, 1995) have been widely viewed as providing a paradigm for understanding the ligand binding and activation of other members of the hematopoietic receptor superfamily, including the EPO receptor. One of the most significant results of these studies is therefore the fact that the behavior of EPO and its receptor is strikingly different.

The 2:1 complex of hGHbp with hGH appears to be much more stable and thermodynamically favored than the comparable EPO complex. For example, SEC studies of mixtures of hGHbp and hGH at 2:1 stoichiometry (Cunningham *et al.*, 1991) appear to show 100% 2:1 complex (based on elution positions) at protein concentrations somewhat below those where the 2:1 sEPOR:EPO complex is dissociating (Figure 2A, trace 2). Further, 1:1 hGHbp/hGH mixtures show substantial amounts of 2:1 complex by SEC under conditions where only 1:1 complexes occur for sEPOR/EPO. Titration calorimetry data for hGHbp + hGH (Cunningham *et al.*, 1991) are also strikingly different from those in Figures 6 and 7. When hGH is added to hGHbp, the titration ends sharply at 0.5 equiv of hGH per hGHbp, and no binding response (neither endo- nor exothermic) is seen through the region of 0.5:1 to 1:1 stoichiometry where the endothermic phase is seen for EPO + sEPOR. The binding of hGHbp to hGH also releases 5−6 times more heat than sEPOR binding to EPO.

A two-site, sequential binding mechanism has been proposed for hGHbp binding to hGHbp to explain structural, binding, and mutagenesis data (de Vos *et al.*, 1992; Cunningham *et al.*, 1991; Fuh *et al.*, 1992). The binding of the first hGHbp to hGH at site 1 occurs with high affinity ($K_d$ ~ 0.3 nm) and involves extensive surface contacts between receptor and hormone. The binding of the second hGHbp to site 2 involves fewer contacts with hGH (and presumably less binding energy) but is further stabilized by significant contacts between the two receptors. Because hGH mutations which significantly reduce the site 1 affinity also seem to eliminate binding to site 2, it has been proposed that binding is sequential, with no binding to site 2 until site 1 is occupied (presumably because the additional receptor−receptor interaction is needed to stabilize binding to site 2). While no

$K_d$ measurement for site 2 in hGH has been reported, the available data suggest that binding of a second hGHbp when site 1 is occupied occurs with an affinity comparable to that for site 1 binding. One aspect of the hGH model which has yet to be explained is the apparent absence of receptor−receptor interactions when no hGH is bound (since the site of these interactions is remote from the hGH binding site, there is no obvious structural reason why this interaction should require site 1 to be occupied).

Overall, the differences between EPO and hGH seem to primarily arise from a much weaker site 2 interaction for EPO. Whether these differences are merely quantitative, or also involve a qualitative change in mechanism, is not entirely clear. The affinity for binding the second hGHbp to hGH is due to both hormone−receptor and receptor−receptor bonds. Assuming the same mechanism exists for EPOR + EPO, it would be interesting to know whether the low affinity of site 2 is due to a weak receptor−ligand bond or due to poor receptor−receptor interactions. We have been able to explain all the data for sEPOR + EPO using a model with two independent binding sites. However, as noted earlier, these data are also compatible with the sequential binding model, because when the two binding sites have very different affinities it makes little difference whether or not site 2 exists when site 1 is unoccupied. Another factor which makes it hard to compare EPO and hGH in detail is the fact that corresponding data and analytical methods are not available for both systems, particularly sedimentation equilibrium data. For both systems, it would be interesting to use sedimentation equilibrium to look for possible weak site 2 binding by mutant ligands which abrogate the site 1 interaction and conversely to try to quantitate the receptor−receptor interactions predicted by the sequential model using mutant ligands which lack site 2 receptor−ligand interactions.

*Relation to EPO Binding and Signal Transduction in Vivo.* These studies have shown definitively that the EPO receptor extracellular domain is capable of producing receptor dimerization in the presence of EPO and thus are consistent with a view that receptor dimerization is both necessary and sufficient to initiate signal transduction. However, it is difficult to reconcile certain features of the data for sEPOR with what is known about the activity of EPO *in vivo* and on cells expressing EPOR *in vitro*. In particular, the low affinity of the site 2 interaction might seem to be insufficient to dimerize the holoreceptor on cells. However, the dimerization of EPOR in a cell membrane is fundamentally a different event than in solution. Thus, to ask whether the ~2 $\mu$M site 2 dissociation constant measured for sEPOR and CHO EPO free in solution will provide sufficient affinity to induce receptor dimerization on a cell will require converting the solution affinities into an appropriate membrane context.

First, if we assume that the intrinsic molecular interactions of the holoreceptor with EPO are the same as those of sEPOR, then the lower translational and rotational entropy of proteins confined to a membrane will make the binding of a second receptor to a 1:1 receptor:EPO complex (a diffusional event within the membrane) more favorable energetically by $^3/_2RT$, increasing the affinity for this process 4.5-fold over that seen in solution. Next we must somehow relate the two-dimensional concentration of receptors in a membrane to their effective molar concentration in three dimensions. This is usually done by assuming the receptors occupy an effective volume corresponding to the area of the cell membrane times its thickness (Lauffenburger & Linderman, 1993).[3] Assuming EPO-dependent cells typically have 500−2000 receptors/cell (Sawyer, 1994b; Takahashi *et al.*, 1995), a cell diameter of ~10 $\mu$m, and a membrane thickness of ~10 nm and that the receptors are uniformly distributed over the cell surface, the effective concentration of EPOR is ~250−1000 nM. This concentration is therefore comparable to the $K_d$ of ~400 nM expected for site 2 in a 1:1 complex bound to the membrane, implying that at least some receptor dimerization will occur.

These calculations are illustrated more clearly in Figure 8A, where we have translated fixed $K_d$'s of 1 nM and 2 $\mu$M from the solution to membrane context for sites 1 and 2, respectively, and used a sequential binding model to calculate the fractional dimerization of EPO receptors in a membrane over a wide range of EPO concentrations and receptor densities on the cell surface. If 1000 receptors are uniformly distributed over a 10 $\mu$m diameter cell, we would expect the behavior shown in trace B, where at most ~20% of the receptors are dimerized even at high EPO concentrations, and only ~1 receptor dimer/cell would be expected at the ~1 pM concentrations which are sufficient for significant activity *in vivo* and *in vitro*.

Thus, these calculations suggest that the binding interactions of the receptor alone may be insufficient to explain receptor dimerization by EPO under physiological conditions. However, there are several effects we have not yet considered which would lead to substantially greater receptor dimerization. First, the distribution of receptors in the membrane may well be nonuniform. A clustering of receptors that increases the local density by 10-fold would, for example, produce receptor dimerization equivalent to that in Figure 8A, curve C. Second, even very weak interactions between the transmembrane or intracellular portions of the receptor would have a dramatic effect. For example, if such interactions gave a very weak homodimerization of the receptor equivalent to a solution $K_d$ of 50 mM (−1.8 kcal/mol binding energy), this would enhance dimerization 100-fold and give a behavior like that in curve D even at 1000 receptors/cell. Lastly, another factor that would strongly influence the overall behavior is the possible presence of substantial amounts of disulfide-linked EPOR oligomers as reported by Miura and Ihle (1993b).

It is also important to note that only a small fraction of receptors may need to be dimerized to obtain a maximal biological response. Indeed, Figure 8 illustrates that, unless this is true, the biological response to EPO should be strongly inhibited at high doses (a self-antagonist effect). The actual proliferative and colony-forming activity of EPO on cells does not decrease significantly even at concentrations which are ~100 times greater than that necessary for saturation of the biological response (Imai *et al.*, 1990). For human growth hormone, self-antagonism has been reported, but only at concentrations ~10000-fold higher than needed for saturation of the growth response (Fuh *et al.*, 1992).

Overall, this analysis suggests that the binding affinity of sEPOR is, at best, marginally sufficient to explain EPO's biological activity, unless there is significant clustering of the receptors on the cell surface, unless dimerization of EPOR on a cell is enhanced by the presence of the

[3] If we instead calculate the effective concentration as that concentration which gives a mean distance between molecules equivalent to that of 500−2000 receptors on a cell, that concentration range is 150−600 nM.

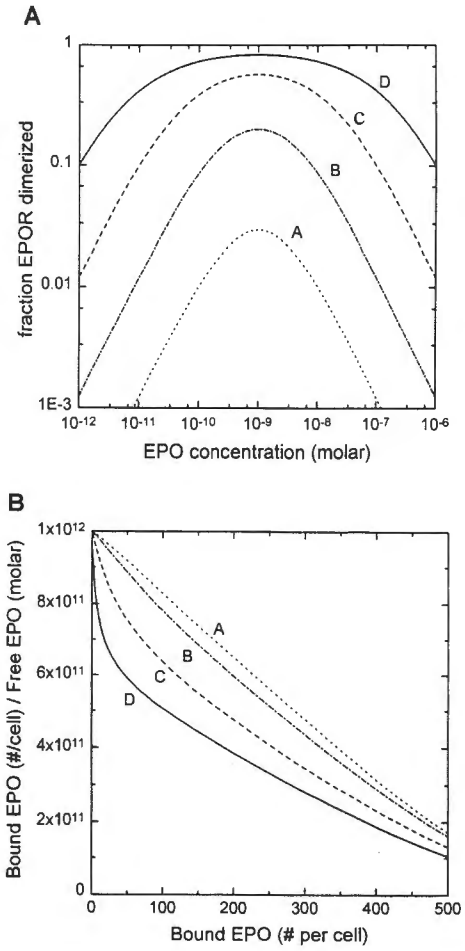


FIGURE 8: Theoretical effect of EPO concentration on receptor dimerization and EPO binding with membrane-bound receptor and a sequential binding model. Values were calculated with a fixed site 1 dissociation constant of 1 nM and a fixed site 2 dissociation constant of 2 $\mu$M (when measured for soluble receptor). Methods for relating binding affinities in solution to two-dimensional binding within a membrane are described in the text. In panel A, the fraction of EPOR dimerized is shown as a function of the number of receptors per cell (assumed to be uniformly distributed over the surface of a 10 $\mu$m diameter cell). The receptors/cell are (A) 100, (B) 1000, (C) 10 000, and (D) 100 000. Panel B shows a Scatchard plot of the total amount of EPO bound to both EPOR monomers and dimers using the same model, affinities, and receptor densities as in panel A, but the membrane area/cell is varied to keep the total number of receptors at 1000 per cell (which makes the scales of Scatchard plots at different receptor densities directly comparable). Therefore, all the curves in panel B intersect the $x$-axis at 1000 EPO per cell. For both panels, equivalent binding curves would be seen with lower receptor densities if the site 2 dissociation constant were lowered proportionally, or if there are any additional interactions between the transmembrane or intracellular portions of the receptor. Virtually identical results would be obtained for the two independent binding sites model, where site 2 is active for binding even when site 1 is unoccupied.

transmembrane and intracellular domains, or unless dimerization is enhanced by other cellular components.

*Relation to High-Affinity and Low-Affinity Classes of Cell Surface Receptors.* Both high-affinity ($K_d \leq 0.1$ nM) and low-affinity ($K_d = 0.2-2$ nM) binding sites for EPO have often been reported on cells expressing the EPO receptor, and much emphasis has been placed on the significance of this phenomenon. For example, it has been suggested that the two classes of receptors are correlated with whether a cell responds to EPO only by growth or also by differentiation and that high-affinity sites are created by the presence of another cellular component along with EPOR (Dong & Goldwasser, 1993; Masuda *et al.*, 1993; Nagao *et al.*, 1993). All studies of the EPO receptor extracellular domain, including this study, are consistent with its classification as a low-affinity receptor.

Now that it is definitively established that EPO is bivalent toward its receptor, however, a re-examination of the concept of two affinity classes and the significance of nonlinear Scatchard plots for EPO binding to cells is worthwhile. Given that EPO is bivalent, whenever binding studies are done under conditions where the receptor is being dimerized, a Scatchard analysis should (indeed theoretically must) show nonlinear behavior, even if all the receptors are behaving identically. It is well-known that when the binding of a multivalent ligand is measured by Scatchard analysis what one measures is an avidity constant and that the apparent avidity varies with the extent of ligand binding (Lauffenburger & Linderman, 1993). Depending on the local density of receptors, the initial slope on a Scatchard plot can imply a dissociation constant ranging from that of site 1 alone (~1 nM) to as small as the product of the site 1 and 2 dissociation constants (<1 fM based on these data for sEPOR). This avidity effect is illustrated in Figure 8B, a Scatchard plot for the same binding model and data used in Figure 8A. This illustrates how multivalent binding to EPO will generate nonlinear Scatchard plots, which could easily be misinterpreted as showing two classes of sites. Further, Figure 8B illustrates how these avidity effects can easily account for Scatchard plots that imply affinities well below the site 1 dissociation constant, without any need to invoke the presence of other components to increase binding affinity.

If thermodynamics predicts that EPO binding should always give nonlinear Scatchard plots when EPOR is being dimerized (and independently of any specific binding model), then why are simple linear plots often reported? There are several effects that might mask the expected nonlinear behavior. First, in many such cases, the reported $K_d$ is not much different than the intrinsic site 1 $K_d$ (Sawyer *et al.*, 1987; Watowich *et al.*, 1992; Masuda *et al.*, 1993; Miura & Ihle, 1993a; Hilton *et al.*, 1995), so little nonlinearity is expected (as in Figure 8B, curves A and B). The need to correct for nonspecific binding (which is often substantial, especially at EPO concentrations needed to see relatively low-affinity binding), and the inherent noise and error in such measurements, may make a truly nonlinear curve appear linear within measurement error. This probably cannot, however, account for reports of single classes of high affinity sites (Todokoro *et al.*, 1987; Damen *et al.*, 1992; Takahashi *et al.*, 1995). Third, EPO will dissociate much more rapidly from any 1:1 complexes that may be present. Such dissociation may occur during washing and separation steps, favoring detection of only the more stable, higher-avidity 2:1 complexes.

Multivalent binding by EPO also predicts that the apparent avidity of EPOR should be different in different cell types due to differences in either the number or distribution of receptors. Is there any experimental evidence for this phenomenon? To our knowledge, this has not yet been systematically studied, and it is difficult to know whether the receptors are uniformly distributed or whether a given cell type contains other components that might influence the binding. We would probably most clearly see this effect when EPOR is heavily overexpressed in a cell line not responsive to EPO. Indeed, when murine EPOR was transfected into COS cells at ~$2 \times 10^5$ receptors/cell, it was

reported to exhibit two binding classes with $K_d$s of 30 and 210 pM for human EPO (D'Andrea *et al.*, 1989). In contrast, the same laboratory later reported a single class with $K_d$ = 750 pM for COS expression at $9 \times 10^3$ receptors/cell (Hilton *et al.*, 1995), suggesting that high receptor density does lead to the appearance of high-affinity sites. However, Miura and Ihle (1993a) reported a single class with $K_d$ = 860 pM at $3.8 \times 10^4$ receptors/cell in COS, a density where we would expect both some nonlinearity and a higher avidity. An exact comparison of these results with Figure 8B is complicated by the fact that human EPO exhibits 4−5-fold poorer biological activity and binding with the murine than the human receptor (Elliott *et al.*, 1993), but the apparent lack of strong avidity effects at $\sim 10^4$ receptors/cell does suggest that there are not significant additional receptor−receptor interactions mediated by the transmembrane or intercellular domains, at least for the murine receptor.

It is certainly also true that both high- and low-affinity sites are often reported in EPO-responsive cell lines with only 100−1000 receptors/cell (Fukamachi *et al.*, 1987; Krantz *et al.*, 1988; Masuda *et al.*, 1993; Nagao *et al.*, 1993). As noted above, we would not predict a strong avidity effect at these receptor densities unless the receptors are strongly clustered or there are additional interactions in the holoreceptor or with other components in these cells. Further, Dong and Goldwasser (1993) have reported that a 10-fold amplification of expression of EPOR in CHO cells leads to an increase in low-affinity sites, but no increase in high-affinity sites, and that fusing together a cell type containing only low-affinity sites with nontransfected CHO cells leads to the appearance of high-affinity EPO sites. They interpreted both these results as indicating that CHO cells constitutively express a limited amount of an accessory component that alters the binding affinity of EPOR. We believe an alternate interpretation is that these results may instead reflect changes in avidity and a limited amount of a component that either clusters EPOR or which alters interactions between the EPOR transmembrane or intercellular domains.

The main point of this discussion is that, given the intrinsic avidity effects that arise from multivalent binding, it is very difficult to distinguish whether nonlinear Scatchard plots truly reflect multiple classes of binding sites or whether the appearance of high-affinity sites truly indicates the presence of new interactions. Overall, it is our view that the possible participation of additional proteins in a hetero-oligomeric complex with EPOR and EPO remains an open question but that it is now clear that no third component is required for EPO to dimerize EPOR.

## ACKNOWLEDGMENT

We thank Vann Parker for expressing sEPOR in CHO cells and Thomas Strickland, Steven Elliott, and Joan Egrie for their support and helpful discussions.

## REFERENCES

Arakawa, T., Wen, J., & Philo, J. S. (1994) *Arch. Biochem. Biophys. 308*, 267−273.

Clackson, T., & Wells, J. A. (1995) *Science 267*, 383−386.

Cunningham, B. C., Ultsch, M., de Vos, A. M., Mulkerrin, M. G., Clauser, K. R., & Wells, J. A. (1991) *Science 254*, 821−825.

Damen, J., Mui, A. L.-F., Hughes, P., Humphries, K., & Krystal, G. (1992) *Blood 80*, 1923−1932.

D'Andrea, A. D., Lodish, H. F., & Wong, G. G. (1989) *Cell 57*, 277−285.

Davis, J. M., Arakawa, T., Strickland, T. W., & Yphantis, D. A. (1987) *Biochemistry 26*, 2633−2638.

de Vos, A. M., Ultsch, M., & Kossiakoff, A. A. (1992) *Science 255*, 306−312.

Dong, Y. J., & Goldwasser, E. (1993) *Exp. Hematol. 21*, 483−486.

Elliott, S. G., Chang, D., DeLorme, E., & Lorenzini, T. (1993) *J. Cell. Biochem. S17B*, 89.

Fuh, G., Cunningham, B. C., Fukunaga, R., Nagata, S., Goeddel, D. V., & Wells, J. A. (1992) *Science 256*, 1677−1680.

Fukamachi, H., Saito, T., Tojo, A., Kitamura, T., Urabe, A., & Takaku, F. (1987) *Exp. Hematol. 15*, 833−837.

Gill, S. J., & von Hippel, P. H. (1989) *Anal. Biochem. 182*, 319−326.

Heldin, C.-H. (1995) *Cell 80*, 213−223.

Hilton, D. J., Watowich, S. S., Murray, P. J., & Lodish, H. F. (1995) *Proc. Natl. Acad. Sci. U.S.A. 92*, 190−194.

Ihle, J. N., Witthuhn, B. A., Quelle, F. W., Yamamoto, K., Thierfelder, W. E., Kreider, B., & Silvennoinen, O. (1994) *Trends Biochem. Sci. 19*, 222−227.

Imai, N., Kawamura, A., Higuchi, M., Oh-eda, M., Orita, T., Kawaguchi, T., & Ochi, N. (1990) *J. Biochem. 107*, 352−359.

Klingmüller, U., Lorenz, U., Cantley, L. C., Neel, B. G., & Lodish, H. F. (1995) *Cell 80*, 729−738.

Krantz, S. B., Sawyer, S. T., & Sawada, K.-I. (1988) *Br. J. Cancer 58* (Suppl. IX), 31−35.

Laue, T. M., Shah, B. D., Ridgeway, T. M., & Pelletier, S. L. (1992) in *Analytical Ultracentrifugation in Biochemistry and Polymer Science* (Harding, S. E., Rowe, A. J., & Horton, J. C., Eds.) pp 90−125, Royal Society of Chemistry, Cambridge.

Lauffenburger, D. A., & Linderman, J. J. (1993) in *Receptors: Models for Binding, Trafficking, and Signalling*, pp 144−167, Oxford University Press, New York.

Masuda, S., Nagao, M., Takahata, K., Konishi, Y., Gallyas, F., Jr., Tabira, T., & Sasaki, R. (1993) *J. Biol. Chem. 268*, 11208−11216.

Miura, O., & Ihle, J. N. (1993a) *Blood 81*, 1739−1744.

Miura, O., & Ihle, J. N. (1993b) *Arch. Biochem. Biophys. 306*, 200−208.

Miura, O., Miura, Y., Nakamura, N., Quelle, F. W., Witthuhn, B. A., Ihle, J. N., & Aoki, N. (1994) *Blood 84*, 4135−4141.

Miyajima, A., Mui, A. L.-F., Ogorochi, T., & Sakamaki, K. (1993) *Blood 82*, 1960−1974.

Nagao, M., Masuda, S., Abe, S., Masatsugu, U., & Sasaki, R. (1992) *Biochem. Biophys. Res. Commun. 188*, 888−897.

Nagao, M., Matsumoto, S., Masuda, S., & Sasaki, R. (1993) *Blood 81*, 2503−2510.

Narhi, L. O., Arakawa, T., Aoki, K. H., Elmore, R., Rohde, M. F., Boone, T., & Strickland, T. W. (1991) *J. Biol. Chem. 266*, 23022−23026.

Philo, J. S., Talvenheimo, J., Wen, J., Rosenfeld, R., Welcher, A., & Arakawa, T. (1994) *J. Biol. Chem. 269*, 27840−27846.

Sawyer, S. T. (1994a) *Blood 84*, 426A.

Sawyer, S. T. (1994b) *Ann. N.Y. Acad. Sci. 718*, 185−190.

Sawyer, S. T., Krantz, S. B., & Goldwasser, E. (1987) *J. Biol. Chem. 262*, 5554−5562.

Takagi, T. (1990) *J. Chromatogr. 280*, 409−416.

Takahashi, T., Chiba, S., Hirano, N., Yazaki, Y., & Hirai, H. (1995) *Blood 85*, 106−114.

Takeuchi, M., Inoue, N., Strickland, T. W., Kubota, M., Wada, M., Shimizu, R., Hoshi, S., Kozutsumi, H., Takasaki, S., & Kobata, A. (1989) *Proc. Natl. Acad. Sci. U.S.A. 86*, 7819−7822.

Todokoro, K. (1994) *Biochem. Biophys. Res. Commun. 203*, 1912−1919.

Todokoro, K., Kanazawa, S., Amanuma, H., & Ikawa, Y. (1987) *Proc. Natl. Acad. Sci. U.S.A. 84*, 4126−4130.

Watowich, S. S., Yoshimura, A., Longmore, G. D., Hilton, D. J., Yoshimura, Y., & Lodish, H. F. (1992) *Proc. Natl. Acad. Sci. U.S.A. 89*, 2140−2144.

Watowich, S. S., Hilton, D. J., & Lodish, H. F. (1994) *Mol. Cell. Biol. 14*, 3535−3549.

Witthuhn, B. A., Quelle, F. W., Silvennoien, O., Yi, T., Tang, B., Miura, O., & Ihle, J. N. (1993) *Cell 74*, 227−236.

Yet, M.-G., & Jones, S. S. (1993) *Blood 82*, 1713−1719.

Yi, T., Zhang, J., Miura, O., & Ihle, J. N. (1995) *Blood 85*, 87−95.

BI9524272